



# $\alpha$ 1-Adrenoceptor Subtype Selectivity: Molecular Modelling and Theoretical Quantitative Structure–Affinity Relationships

P. G. De Benedetti,<sup>a,\*</sup> F. Fanelli,<sup>a</sup> M. C. Menziani,<sup>a</sup> M. Cocchi,<sup>a</sup> R. Testa,<sup>b</sup> and A. Leonardi<sup>b</sup>

<sup>a</sup>*Dipartimento di Chimica, Università di Modena, Via Campi 183, 41100 Modena, Italy*

<sup>b</sup>*Farmaceutical R&D Division Recordati S.p.A., via Civitali 1, 20148 Milan, Italy*

**Abstract**—This study constitutes a preliminary rationalization, at the molecular level, of antagonist selectivity towards the three cloned  $\alpha$ 1-adrenergic receptor ( $\alpha$ 1-AR) subtypes. Molecular dynamics simulations allowed a structural/dynamics analysis of the seven  $\alpha$ -helix-bundle models of the bovine  $\alpha$ 1a-, hamster  $\alpha$ 1b-, and rat  $\alpha$ 1d-AR subtypes. The results showed that the transmembrane domains of these subtypes have different dynamic behaviours and different topographies of the binding sites, which are mainly constituted by conserved residues. In particular, the  $\alpha$ 1a-AR binding site is more flexible and topographically different with respect to the other two subtypes. The results of the theoretical structural/dynamics analysis of the isolated receptors are consistent with the binding affinities of the 16 antagonists tested towards the three cloned  $\alpha$ 1-AR subtypes. Moreover, the theoretical quantitative structure–affinity relationships obtained from the antagonist–receptor interaction models further corroborates the hypothesis that selectivity towards one preferential subtype is mainly modulated by receptor and/or ligand distortion energies. In other words, subtype selectivity seems to be mainly guided by the dynamic complementarity (induced fit) between ligand and receptor. On the basis of the quantitative models presented it is possible to predict both affinities and selectivities of putative  $\alpha$ 1-AR ligands as well as to estimate the theoretical  $\alpha$ 1-AR subtype affinities and selectivities of existing antagonists. © 1997 Elsevier Science Ltd.

## Introduction

Drug selectivity towards different target receptors is a challenging problem, which is further complicated by the continuous identification of new receptor families and new receptor subtypes inside the same family. This process imposes a frequent updating of the pharmacological classification of the ligands as well as of their structure–activity relationships (SAR). In this context,  $\alpha$ -adrenergic receptors ( $\alpha$ -AR) constitute a very representative example. The subclassification of the  $\alpha$ -AR into the  $\alpha$ 1 and  $\alpha$ 2 subtypes<sup>1,2</sup> made possible the development of effective antihypertensive drugs that either selectively block the  $\alpha$ 1-AR or activate the  $\alpha$ 2-AR subtype. About 10 years after this subclassification, the first suggestion for further subdivisions was made on the basis of functional and radioligand binding data.<sup>3–5</sup> Currently, the presence of at least three  $\alpha$ 1-AR subtypes ( $\alpha$ 1a,  $\alpha$ 1b and  $\alpha$ 1d) has been established by means of molecular biology, radioligand binding and functional studies.<sup>6–11</sup> The functional evidence of further distinct subtypes showing low affinity for prazosin is still awaiting confirmation from molecular biology.<sup>12–14</sup>

The study of drug selectivity is now approachable by means of molecular modelling procedures, which help elucidate the three-dimensional (3-D) molecular determinants of ligand affinity/selectivity.

Recently, we proposed a novel theoretical quantitative structure–activity relationship (QSAR) approach

named heuristic direct.<sup>15–20</sup> This approach, applicable when the atomic resolved structure of the target is unknown but predictable by means of the available experimental information, is able to handle the heterogeneous experimental data on the ligands and their targets and to synthesize and translate them into QSAR models. The first step of this procedure consists of the computer-aided 3-D model building of the receptor. The second step involves docking simulations with selected ligands, maximizing the complementarity between ligand and receptor. In the final step, a detailed, extensive correlation analysis between the computed intermolecular interaction descriptors and the experimental binding affinities is carried out in order to evaluate the consistency of the QSAR model proposed. In the present work, the heuristic direct approach has been applied to the study of selectivity of various antagonists towards the cloned bovine  $\alpha$ 1a-, the hamster  $\alpha$ 1b-, and the rat  $\alpha$ 1d-ARs. The results of this study have been presented in terms of comparative analyses that have been performed at three different levels. Firstly, the three  $\alpha$ 1-AR subtypes have been compared in their primary sequences. Secondly, the seven  $\alpha$ -helix bundle models of the three AR subtypes have been compared in their structure/dynamic features. Finally, the minimized average structures of the three subtypes have been compared in their interaction modes with 16 non-selective and subtype-selective antagonists. In this context, ligand/receptor docking simulations have allowed us to compute theoretical intermolecular interaction descriptors that help to

rationalize the antagonist binding affinities measured on the three cloned receptors.

The results of this work provide an explanation, at the molecular level, of antagonist selectivity towards the  $\alpha 1$ -AR subtypes.

## Results and Discussion

This theoretical study focuses on the transmembrane (TM) domains of the bovine  $\alpha 1a$ -,<sup>8</sup> hamster  $\alpha 1b$ -,<sup>7</sup> and rat  $\alpha 1d$ -AR<sup>6</sup> subtypes. The TM primary sequences of these  $\alpha 1$ -ARs are aligned in Chart 1. The squared sequences refer to the extracellular half of TM domains that contain the putative ligand binding site. The amino acids that differ only in one subtype are typed in bold, whereas the amino acids that differ within all the three subtypes are shadowed. By comparing these sequences it is seen that (a) the TM domains of the  $\alpha 1a$ -AR and the  $\alpha 1b$ -AR differ for 47 amino acids (27 lie in the extracellular half); (b) the TM domains of the  $\alpha 1a$ -AR and the  $\alpha 1d$ -AR differ for 59 amino acids (31 lie in the extracellular half); and (c) the TM domains of the  $\alpha 1b$ -AR and the  $\alpha 1d$ -AR differ for 47 amino acids (22 lie in the extracellular half). The TM domain of the  $\alpha 1a$ -AR

subtype shows the lowest degree of homology with respect to the other two subtypes.

To compare the structural/dynamic features of these domains we have performed molecular dynamics (MD) simulations on the seven  $\alpha$ -helix bundle models of the three subtypes and we have considered the structures averaged over the last 100 ps of the equilibrated simulation time period. From the topographical analysis of the three minimized average structures the following observations can be made. (a) Among the amino acids that differ between the  $\alpha 1a$ -AR and the  $\alpha 1b$ -AR subtypes, 16 are directed towards the phospholipid bilayer and the others mainly lie in interhelical positions. The four non-conserved residues are directed towards the receptor core in the environments of D3:07, which is the putative key residue for the cationic ligand/receptor recognition,<sup>21</sup> and lie in positions 2:14, 5:07, 6:20, and 7:06 (Chart 1). (b) Among the amino acids that differ between the  $\alpha 1a$ -AR and the  $\alpha 1d$ -AR subtypes, 17 are directed towards the phospholipid bilayer and the other mainly lie in interhelical positions. There are four putative binding site residues non-conserved between these two subtypes and they lie at the same positions as the putative binding site residues non-conserved between the  $\alpha 1a$  and the  $\alpha 1b$ -AR

	HELIX 1																									
bovine $\alpha 1a$	A	I	L	L	G	V	I	L	G	G	L	I	L	F	G	V	L	G	N	I	L	V	I	L	S	V
hamster $\alpha 1b$	A	I	S	V	G	L	V	L	G	A	F	I	L	F	A	I	V	G	N	I	L	V	I	L	S	V
rat $\alpha 1d$	G	V	G	V	G	V	F	L	A	A	F	I	L	T	A	V	A	G	N	L	L	V	I	L	S	V
	HELIX 2																									
bovine $\alpha 1a$	Y	Y	I	V	N	L	A	V	A	D	L	L	L	T	S	T	V	L	P	F	S	A	I	F	E	I
hamster $\alpha 1b$	Y	F	I	V	N	L	A	I	A	D	L	I	L	S	F	T	V	L	P	F	S	A	T	L	E	V
rat $\alpha 1d$	Y	F	I	V	N	L	A	V	A	D	L	L	L	S	A	A	V	L	P	F	S	A	T	M	E	V
	HELIX 3																									
bovine $\alpha 1a$	N	V	W	A	A	V	D	V	L	C	C	T	A	S	I	M	G	L	C	I	I	S	I	D		
hamster $\alpha 1b$	D	I	W	A	A	V	D	V	L	C	C	T	A	S	I	L	S	L	C	A	I	S	I	D		
rat $\alpha 1d$	D	V	W	A	A	V	D	V	L	C	C	T	A	S	I	L	S	L	C	T	I	S	V	D		
	HELIX 4																									
bovine $\alpha 1a$	G	L	M	A	L	L	C	V	W	A	L	S	L	V	I	S	I	G	P	L	F	G	W	R		
hamster $\alpha 1b$	A	I	L	A	L	L	S	V	W	V	L	S	T	V	I	S	I	G	P	L	L	G	W	K		
rat $\alpha 1d$	A	A	A	I	L	A	L	L	W	A	V	A	L	V	V	S	V	G	P	L	L	G	W	K		
	HELIX 5																									
bovine $\alpha 1a$	G	Y	V	L	F	S	A	L	G	S	F	Y	V	P	L	T	I	I	L	V	M	Y	C			
hamster $\alpha 1b$	F	Y	A	L	F	S	S	L	G	S	F	Y	I	P	L	A	V	I	L	V	M	Y	C			
rat $\alpha 1d$	G	Y	A	I	F	S	S	V	C	S	F	Y	L	P	M	A	V	I	V	V	M	Y	C			
	HELIX 6																									
bovine $\alpha 1a$	T	L	G	I	V	V	G	C	F	V	L	C	W	L	P	F	F	L	V	M	P	I	G	S		
hamster $\alpha 1b$	T	L	G	I	V	V	G	M	F	I	L	C	W	L	P	F	F	I	A	L	P	L	G	S		
rat $\alpha 1d$	T	L	A	I	V	V	G	V	F	V	L	C	W	F	P	F	F	F	V	L	P	L	G	S		
	HELIX 7																									
bovine $\alpha 1a$	T	V	F	K	I	A	F	W	L	G	Y	L	N	S	C	I	N	P	I	I	Y	P	C	S		
hamster $\alpha 1b$	A	V	F	K	V	V	F	W	L	G	Y	F	N	S	C	L	N	P	I	I	Y	P	C	S		
rat $\alpha 1d$	G	V	F	K	V	I	F	W	L	G	Y	F	N	S	C	V	N	P	L	I	Y	P	C	S		

Chart 1.

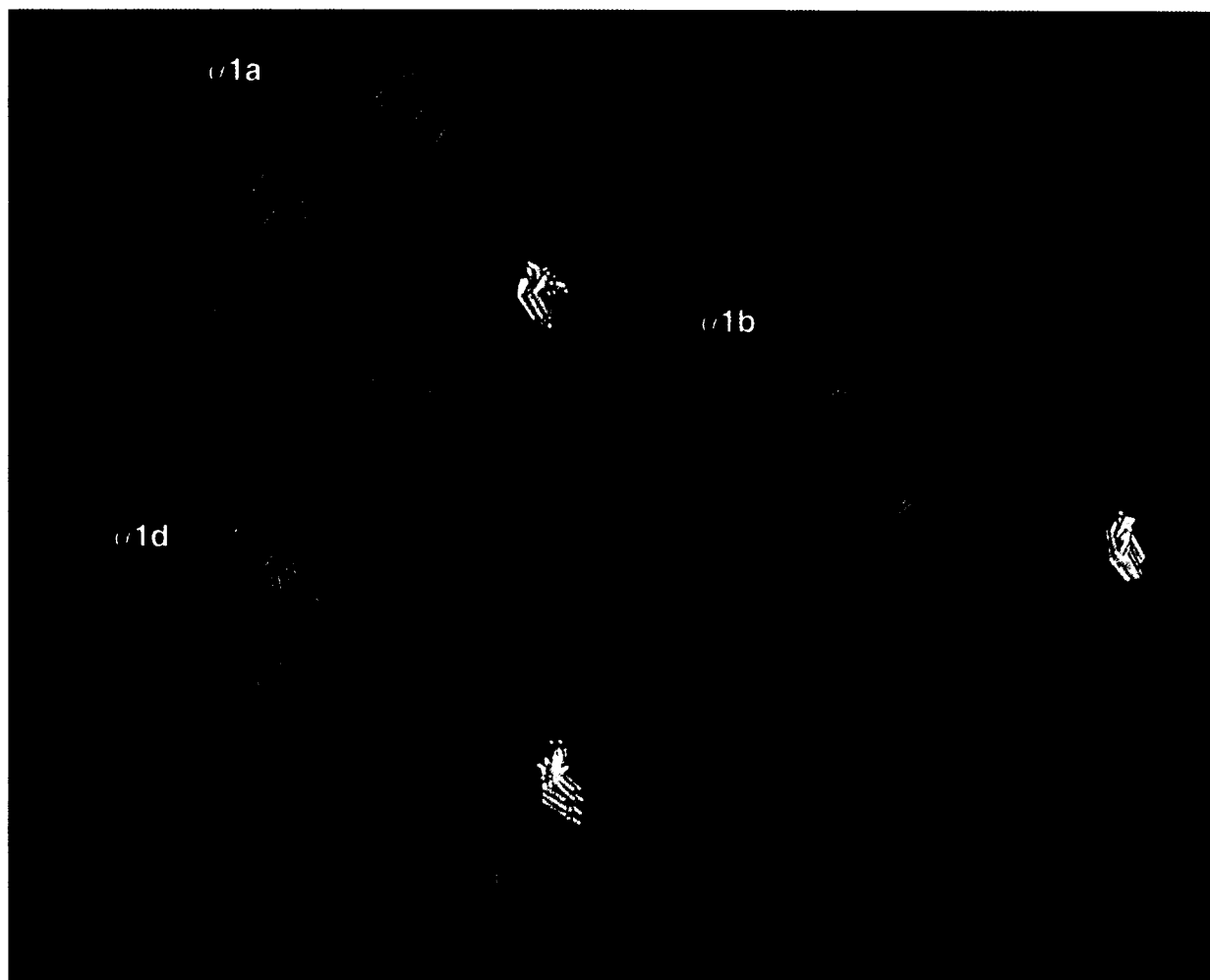


**Figure 1.** Fluctuations of the 'putative' binding site residues of the three  $\alpha$ 1-AR subtypes. The colours orange, green, pink, yellow, light blue, and violet label for TM2, TM3, TM4, TM5, TM6, and TM7, respectively.

subtypes. (c) Among the amino acids that differ between the  $\alpha$ 1b-AR and the  $\alpha$ 1d-AR subtypes, 16 are directed towards the phospholipid bilayer, while the others mainly lie at interhelical positions. The binding sites of these two subtypes differ for only one residue lying at position 7:06.

Assuming that the  $\alpha$ 1-AR antagonists interact in their protonated form with D3:07 (long-range coulombic interactions) as well as with the residues close to this aspartate (short-range intermolecular forces), the topographical distribution of all the amino acids non-conserved among the three  $\alpha$ 1-AR subtypes suggests that they are not directly involved in the interaction with the antagonists and that their main effect might be exerted on the structural/dynamic features of these subtypes. To test this hypothesis we have analysed the MD trajectories of the three  $\alpha$ 1-AR models. By considering several conserved amino acids close to D3:07, we have superimposed 10 putative binding site structures obtained by averaging the coordinates collected over 20 ps time intervals (Fig. 1). Interestingly, we have found that the  $\alpha$ 1a binding site is constituted by

the most fluctuating amino acids and shows a quite different shape with respect to the  $\alpha$ 1b and the  $\alpha$ 1d subtypes. In other words, the  $\alpha$ 1a-AR binding site shows a higher degree of flexibility than the other two subtype binding sites and, hence, is able to accommodate structurally different ligands without incurring significant deviations from the allowed conformational states. These dynamic features are consistent with the pharmacological profile of the antagonists tested on the three cloned receptors (Chart 2). In fact, the binding affinity data values listed in Table 1 show that high affinities for the  $\alpha$ 1-ARs subtypes can be achieved with a structurally heterogeneous series of ligands. In particular, the selectivity for the  $\alpha$ 1a-AR subtype is reached by lowering the affinity for the other two subtypes.

To provide a quantitative description of the above theoretical results, which are based on the structural/dynamic analysis of the free receptor forms, we have docked each of the antagonists listed in Chart 2 into the average minimized structures of the three  $\alpha$ 1-AR subtypes. For each ligand/receptor minimized complex

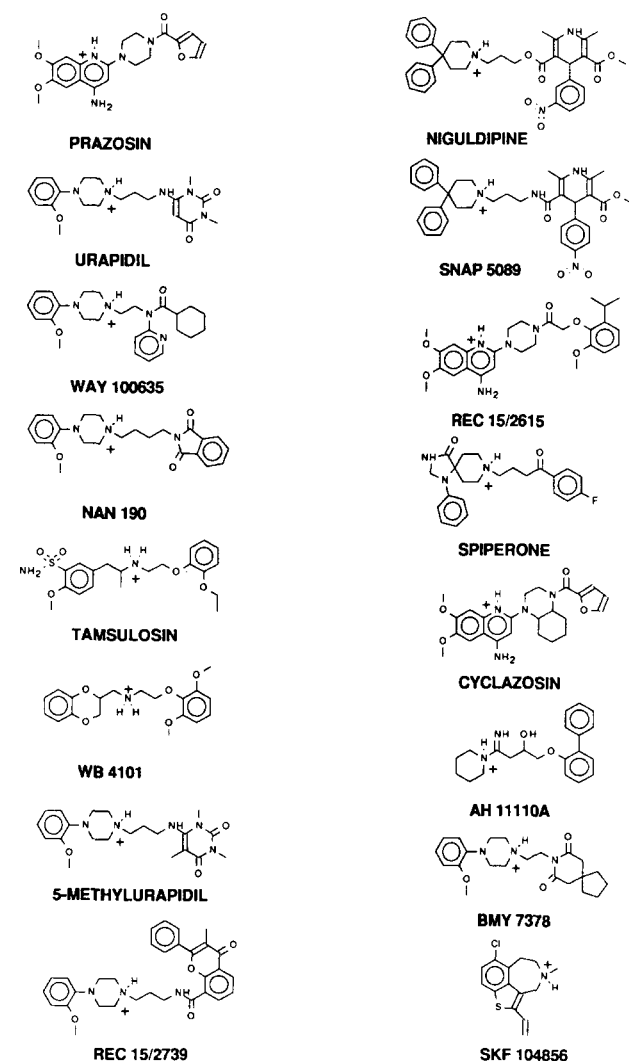


Chart 2.

the theoretical binding energies (BE) have been computed and correlated with the experimental binding affinities measured on the three cloned subtypes; the resulting linear correlations are reported in Figure 2.

The BE of the ligand–receptor minimized complexes have been computed according to the following formula:  $BE = IE + ER + EL$ , where IE is the ligand/receptor interaction energy and ER and EL are the distortion energies of the receptor and of the ligand, respectively, calculated as differences between the energies of the bound and of the free optimized molecular forms. Computed BE values are also reported in Table 1 together with their components, IE, ER, and EL. By analysing this table it results that non-selective antagonists give similar BE values on docking to the three  $\alpha 1$ -AR subtypes, whereas antagonists showing selectivity towards one receptor subtype give lower (energetically favoured) BE values when they are complexed with the preferential target subtype with respect to the other two AR subtypes.

Receptor and ligand distortion energies provide a measure of both ligand and receptor penalties to go from the free to the bound state. In other words, the distortion energies being positive values, the higher the receptor and ligand distortion energies, the lower the ligand/receptor interaction propensity and hence, the lower the ligand–receptor dynamic complementarity.

According to our models, the ‘theoretical  $\alpha 1a$  selectivity’, that is the selectivity encoded by theoretical descriptors, is mainly modulated by receptor and ligand distortion energies. In fact, the interaction energy values computed on the three complexed subtypes are linearly correlated ( $IE1a/IE1b$ :  $r = 0.82$ ;  $IE1a/IE1d$ :  $r = 0.95$ ;  $IE1b/IE1d$ :  $r = 0.85$ ), whereas only the  $\alpha 1b$ -AR and  $\alpha 1d$ -AR distortion energies give a linear trend ( $ER1a/ER1b$ :  $r = 0.44$ ;  $ER1a/ER1d$ :  $r = 0.49$   $ER1b/ER1d$ :  $r = 0.83$ ). In particular, high affinity and selective  $\alpha 1a$ -AR antagonists (WB 4101, Rec 15/2739, S-(+)-niguldipine and SNAP 5089) give similar IE values when they are complexed with the three subtypes, whereas they induce lower distortion energies to the  $\alpha 1a$ -AR than to the other two subtypes (Table 1). The interaction energies modulate the  $\alpha 1b$  selectivity of

**Table 1.** Experimental binding affinities (pK) and computed binding (BE, kcal/mol), interaction (IE, kcal/mol), receptor distortion (ER, kcal/mol), and ligand distortion (EL, kcal/mol) energies of the ligand- $\alpha 1$  adrenoceptor subtype complexes

Compd	pK1a	pK1b	pK1d	BE1a	IE1a	ER1a	EL1a	BE1b	IE1b	ER1b	EL1b	BE1d	IE1d	ER1d	EL1d
Prazosin	9.14	9.34	8.77	-38.80	-77.15	35.00	3.35	-37.44	-90.11	45.64	7.03	-40.96	-78.15	30.37	6.82
Urapidil	6.54	5.88	5.78	-15.99	-82.30	59.27	7.04	-17.79	-83.53	60.84	4.90	-20.27	-85.99	54.27	11.45
WAY 100635	6.84	6.73	7.20	-30.33	-82.13	43.39	8.41	-23.69	-85.73	54.92	7.12	-32.09	-81.12	40.00	9.03
NAN 190	8.70	7.82	9.08	-46.94	-85.31	34.45	3.92	-30.23	-72.91	38.51	4.17	-49.60	-77.19	14.59	13.00
(R)(-)-Tamsulosin	9.82	8.17	8.75	-44.82	-93.04	45.58	2.64	-30.57	-97.98	59.64	7.77	-49.91	-89.03	35.50	3.62
WB 4101	9.21	7.24	8.20	-43.42	-81.85	34.01	4.42	-25.45	-77.81	49.74	2.62	-48.46	-73.02	19.98	4.58
5-Methylurapidil	8.69	5.97	6.30	-36.71	-93.39	52.45	4.23	-16.09	-73.16	51.81	5.26	-17.38	-91.77	58.14	16.25
Rec 15/2739	9.54	7.29	7.60	-44.49	-91.09	42.23	4.37	-27.99	-89.82	56.18	5.65	-29.38	-100.09	58.04	12.67
(S)(+)-Niguldipine	9.42	7.60	7.08	-50.15	-105.51	44.59	10.77	-23.38	-105.70	72.72	9.60	-28.31	-111.58	68.36	14.91
SNAP 5089	9.30	7.12	6.32	-54.91	-107.93	42.36	10.66	-22.00	-105.14	75.05	8.09	-28.71	-109.04	69.70	10.63
Rec 15/2615	8.12	9.35	7.91	-39.42	-92.08	45.56	7.10	-42.15	-95.79	42.80	10.84	-37.44	-94.86	50.81	6.61
Spiiperone	7.87	8.15	7.66	-27.38	-77.66	46.97	3.31	-34.28	-80.67	44.74	1.65	-33.19	-76.41	36.13	7.09
(+)-Cyclazosin	7.48	9.15	7.53	-33.39	-82.23	41.66	7.18	-41.83	-103.87	53.81	8.23	-32.90	-89.03	49.95	6.18
AH 11110A	6.79	7.40	6.42	-15.13	-68.04	49.43	3.48	-20.31	-66.51	42.34	3.86	-25.60	-70.00	34.50	9.90
BMJ 7378	6.30	6.37	8.24	-9.50	-83.36	63.63	10.23	-16.74	-76.00	48.54	10.72	-43.83	-83.12	29.82	9.47
SKF104856	7.36	7.20	8.28	-21.53	-44.28	21.96	0.79	-25.48	-44.96	18.47	1.01	-44.11	-48.14	3.14	0.90

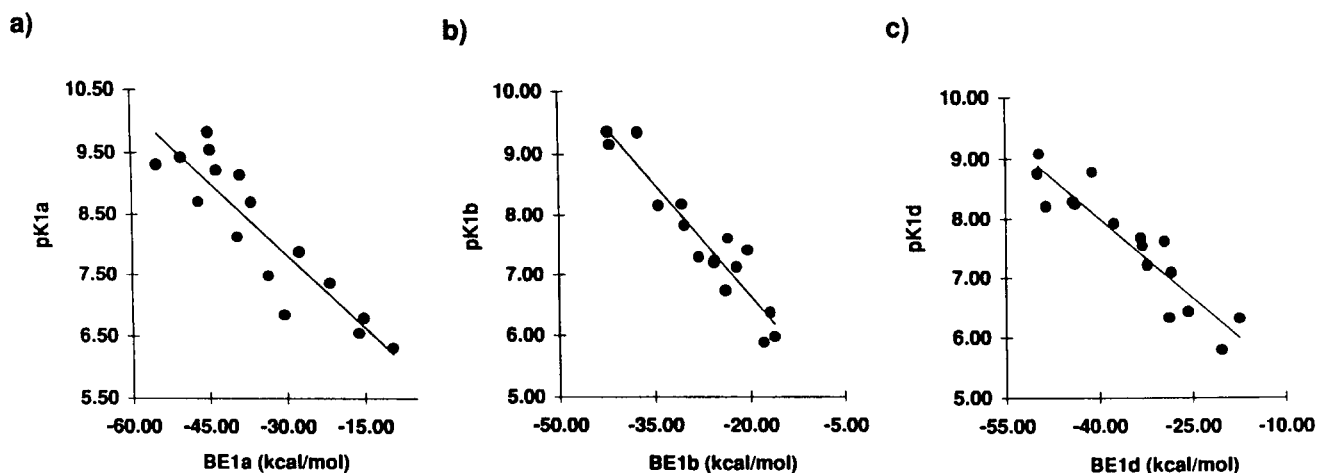


**Figure 2.** Correlations between the experimental binding affinities (pK1a, pK1b, and pK1d) and the computed binding energies (BE1a, BE1b, and BE1d) of the ligand  $\alpha$ 1-adrenoceptor subtype complexes. The linear regression equations are (a)  $pK1a = 5.45 (\pm 0.37) - 0.08 (\pm 0.01) BE1a$ ,  $n = 16$ ,  $r = 0.90$ ,  $s = 0.52$ ; (b)  $pK1b = 4.20 (\pm 0.32) - 0.12 (\pm 0.01) BE1b$ ,  $n = 16$ ,  $r = 0.94$ ,  $s = 0.37$ ; (c)  $pK1d = 4.43 (\pm 0.36) - 0.09 (\pm 0.01) BE1d$ ,  $n = 16$ ,  $r = 0.92$ ,  $s = 0.39$ ; where  $n$  is the number of compounds,  $r$  is the correlation coefficient,  $s$  is the standard deviation, and the number in parentheses give the 95% confidence intervals.

(+)-cyclazosin, whereas distortion energies are the main modulators of  $\alpha$ 1d selectivity of BMY 7378.

Different from these compounds, the antagonist 5-methylurapidil realizes the  $\alpha$ 1a/ $\alpha$ 1b theoretical selectivity by means of its interaction energies, whereas it realizes the  $\alpha$ 1a/ $\alpha$ 1d selectivity by means of the binding energies. In particular, when this antagonist is complexed with the  $\alpha$ 1a-AR it gives an interaction energy value lower (more stable complex) than when it interacts with the  $\alpha$ 1b-AR (Table 1). As it can be seen from Figure 3, the residues interacting with this selective antagonist are mainly conserved among the three subtypes. However, due to the different topographies of the three subtype binding sites, the ligand realizes qualitatively and quantitatively different interaction patterns. In particular, the highly conserved residues which constitute the putative  $\alpha$ 1a ligand-binding site are clustered closer to D3:07 than the corresponding residues in the  $\alpha$ 1b-AR and a greater number of residues are involved in the 5-methylurapidil- $\alpha$ 1a-AR interaction than in the 5-methylurapidil- $\alpha$ 1b-AR interaction; moreover, several conserved residues in the former complex (i.e., D3:07, W6:13, F6:16, F7:07, and Y7:11) give stronger interactions with the antagonist than the same residues in the latter complex.

### Conclusions

The results of this study constitute a preliminary rationalization, at the molecular level, of antagonists' selectivity towards the three  $\alpha$ 1-AR subtypes.

Molecular dynamics simulations allowed a structural/dynamics analysis of the seven  $\alpha$ -helix-bundle models of the bovine  $\alpha$ 1a-, hamster  $\alpha$ 1b-, and rat  $\alpha$ 1d-AR subtypes. The TM domains of the three  $\alpha$ 1-AR subtypes have different dynamic behaviours and different topographies of the putative ligand binding sites,

which are mainly constituted by conserved residues. In particular, the  $\alpha$ 1a-AR binding site is more flexible and topographically different with respect to the other two subtypes. The results of the theoretical structural/dynamics analysis of the isolated receptors are consistent with the binding affinities of the 16 antagonists tested towards the three cloned  $\alpha$ 1-AR subtypes. Moreover, the theoretical quantitative structure-affinity relationships obtained from the antagonist/receptor interaction models further corroborates this hypothesis. In fact, 'theoretical selectivity' towards one preferential subtype seems to be mainly modulated by receptor and/or ligand distortion energies. In other words, subtype selectivity seems to be mainly guided by dynamic complementarity (induced fit) between the ligand and the receptor.

The quantitative models presented allow the prediction of affinities as well as the estimation of the theoretical  $\alpha$ 1-AR subtype affinities and selectivities of existing antagonists.

### Methods

#### 3-D model building of the receptor and docking simulations

The building of the transmembrane (TM) model of the hamster  $\alpha$ 1b-AR subtype was described in detail in our previous paper<sup>22</sup> in which a comparative molecular dynamics (MD) study on the seven helix bundle arrangement of seven G-protein coupled receptors (GPCRs) was presented. Starting from a common topography for the amino acids in the most conserved positions, according to the helical wheel projection models proposed by Baldwin,<sup>23</sup> we arranged the helix bundle in 'bovine-rhodopsin-like'<sup>24</sup> and 'bacteriorhodopsin-like' manners.<sup>25</sup> The bacteriorhodopsin like

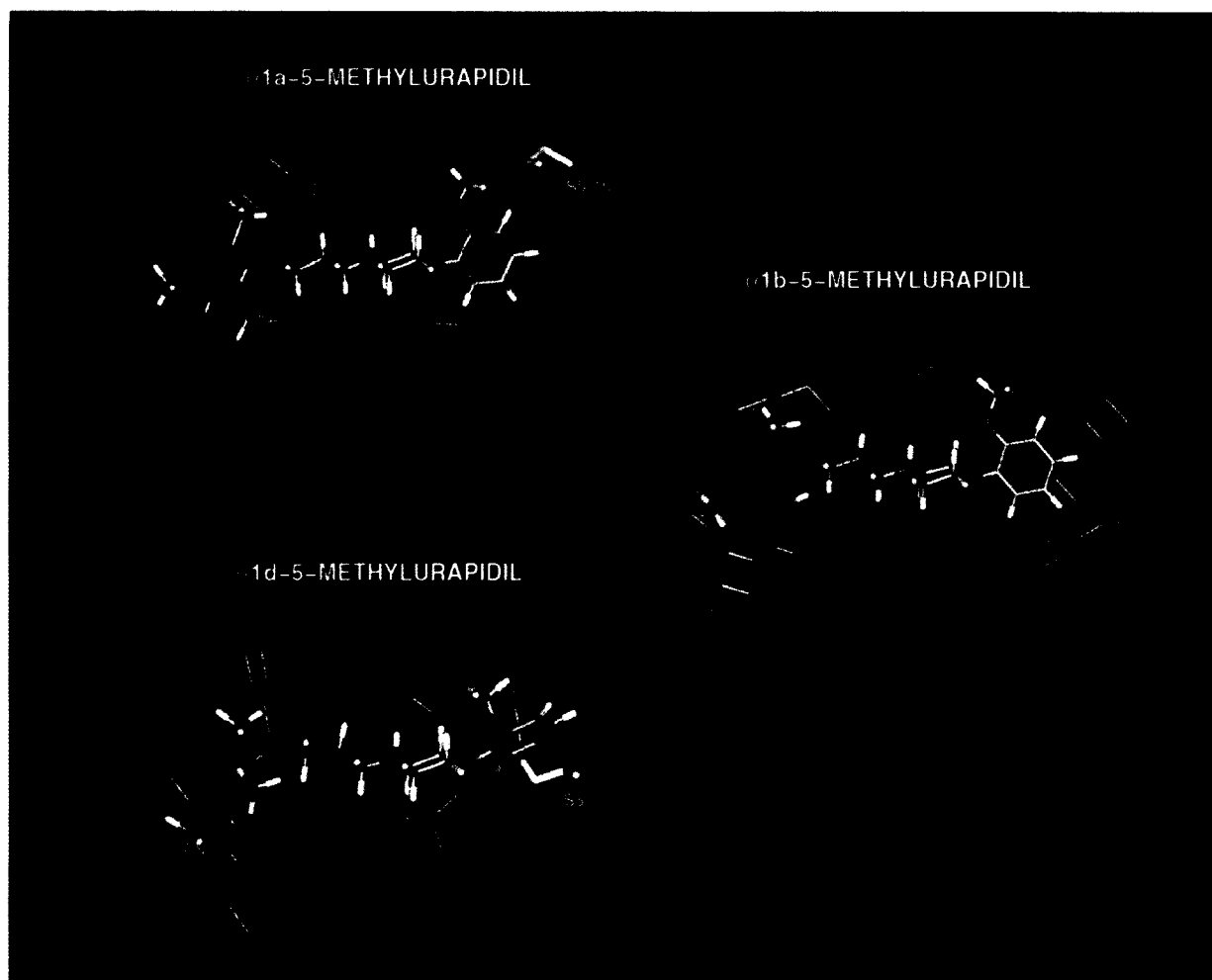


**Figure 3.** Details of the interactions between the  $\alpha1a$ -AR selective antagonist 5-methylurapidil and the three  $\alpha1$ -AR subtypes. The amino acids non-conserved among the three subtypes are indicated by squared labels.

input structure shares with the experimental coordinates of bacteriorhodopsin only the inclination of the helix main axes, the topography of the amino acid positions being almost the same as in the 'bovine-rhodopsin-like' input structure. For each receptor two minimized average structures with a helix bundle arrangement similar to that of the bidimensional projection map of bovine rhodopsin were obtained.<sup>22</sup> This was attributed to the fact that the topography of some fundamental amino acid positions is substantially the same in both the input structures and dictates, through the establishment of similar hydrogen bonding networks, the helix-helix packing.<sup>22</sup> The input structures of the bovine  $\alpha1a$ -AR as well as of the rat  $\alpha1d$ -AR were built by using the backbone coordinates of the  $\alpha1b$ -AR input structure as a template.<sup>22</sup> The initial models were energy minimized and subjected to MD. The structures averaged over the last 100 ps time period of each MD simulation were then minimized.

The input structures of the ligand/receptor complexes were obtained by docking each ligand into the

minimized average structure of its target receptor. For each complex several minimizations were performed in order to probe different orientations of the ligands and optimize several fundamental interactions, that is the charge-reinforced H-bond between the protonated nitrogen atom of the ligands and the carboxylate of D3:07 (the first digit indicates the helix and the last two digits indicate the position of the residues in the helix), which is the putative key residue for the cationic ligand/receptor recognition.<sup>21</sup> In general, the protonated nitrogen atom of all the antagonists makes ionic interactions with the carboxylate of D3:07, whereas the other molecular moieties fit two binding pockets formed by TM1, TM2, and TM7 on one side, and by TM4, TM5, and TM6 on the other one and lying in an almost symmetrical topography with respect to D3:07. The  $\alpha1$ -AR antagonists mainly contain two aromatic moieties on the two sides of the protonated nitrogen atom. In our interaction models, the aromatic moiety closer to the protonated nitrogen atom, docks the hydrophobic pocket formed by residues of TM4, TM5, and TM6.

## Computational procedure

Modelling studies were performed with the molecular graphics package QUANTA (version 4.0).<sup>26</sup> Energy minimizations and MD simulations of the receptors and of the ligand/receptor complexes were obtained by means of the program CHARMM (version 22).<sup>27</sup>

Minimizations were carried out by using 200 steps of steepest descent followed by a conjugate gradient minimization, until the rms gradient was less than 0.001 kcal/mol Å. A distance-dependent dielectric term ( $\epsilon = 4r$ ) and a 12 Å non-bonded cutoff distance were chosen. The 'united atom approximation' was used for computational efficiency.<sup>27</sup>

The minimized coordinates of the three  $\alpha$ 1-AR subtypes were used as the starting point for a 150-ps MD run. The proteins were heated to 300 K with 5 °C rise per 6000 steps by randomly assigning velocities from the Gaussian distribution. After heating, the system was allowed to equilibrate for 34 ps. Velocities were scaled by a single factor. The system was then subjected to 110-ps MD simulation at constant temperature (300 K). The results reported were collected every 0.5 ps from the last 100-ps trajectory. The lengths of the bonds involving hydrogen atoms were constrained according to the SHAKE algorithm,<sup>28</sup> allowing an integration time step of 0.001 ps. The  $\alpha$ -helix conformation was preserved by using the NOE constraint facility of the program with a scaling factor of 10. Integration of Newton's equations of motion was done by using the Verlet algorithm.

The charge distributions of the ligands in their protonated form were obtained in the AM1 framework.<sup>29</sup>

## Radioreceptor binding studies

The affinity of different antagonists for the cloned  $\alpha$ 1-AR subtypes was evaluated by studying their ability to inhibit specific [<sup>3</sup>H]prazosin binding from COS-7 membranes.

Expression of rat  $\alpha$ 1d-, hamster  $\alpha$ 1b-, and bovine  $\alpha$ 1a-ARs was performed as previously described.<sup>6,7,10</sup> The membranes were resuspended in 50 mM Tris-HCl, pH 7.4, containing 10  $\mu$ M pargyline and 0.1% ascorbic acid, quickly frozen, and stored at -70 °C until utilized. The membranes were incubated in 50 mM Tris-HCl, pH 7.4, containing 10  $\mu$ M pargyline and 0.1% ascorbic acid, with 0.3–0.6 nM [<sup>3</sup>H]prazosin, in absence or presence of the displacing drug to be tested over the concentration range 10<sup>-4</sup> to 10<sup>-13</sup> M. Incubation volume was 0.22 mL (35, 35, and 70  $\mu$ g protein/sample for  $\alpha$ 1a,  $\alpha$ 1b, and  $\alpha$ 1d, respectively). Non-specific binding was determined in the presence of 100  $\mu$ M phentolamine. The reaction mixture was incubated for 30 min at 25 °C and then stopped by the addition of ice-cold Tris-HCl buffer and rapid filtration through 0.2% polyethyleneimine pre-

treated Whatman GF/B fibre filters using Brandel cell harvester.

## Acknowledgements

Financial support from the Consiglio Nazionale delle Ricerche (Roma) and Ministero dell'Università e della Ricerca Scientifica (funds 40%) is acknowledged. Technical support from the CICAIA (University of Modena) is acknowledged. We also thank Professor D. Giardinà (University of Camerino) for providing us with the (+)-cyclazosin and Dr J. P. Hieble (SB Pharmaceuticals) for the SKF 104856.

## References

1. Langer, S. Z. *Brit. J. Pharmacol.* **1974**, *60*, 481.
2. Starke, K.; Montel, H.; Gayk, W.; Marker, R. *Naunyn-Schmiedeberg's Arch. Pharmacol.* **1974**, *285*, 133.
3. Flavahan, N. A.; Vanhoutte, P. M. *Trends Pharmacol. Sci.* **1986**, *7*, 347.
4. Morrow, A. L.; Creese, I. *Mol. Pharmacol.* **1986**, *29*, 321.
5. Han, C.; Abel, P. W.; Minneman, K. P. *Nature (London)* **1987**, *329*, 333.
6. Schwinn, D. A.; Lomasney, J. W.; Lorenz, W.; Szklut, P. J.; Fremeau, R. T.; Yang-Feng, T. L.; Caron, M. G.; Lefkowitz, R. J.; Cotecchia, S. *J. Biol. Chem.* **1990**, *265*, 8183.
7. Cotecchia, S.; Schwinn, D. A.; Randall, L. L.; Lefkowitz, R. J.; Caron, M. G.; Kobilka, B. K. *Proc. Natl. Acad. Sci. U.S.A.* **1988**, *85*, 7159.
8. Lomasney, J. W.; Cotecchia, S.; Lorenz, S.; Leung, W.; Schwinn, D. A.; Yang-Feng, T. L.; Brownstein, M.; Lefkowitz, R. J.; Caron, M. G. *J. Biol. Chem.* **1991**, *266*, 6365.
9. Perez, D. M.; Piascik, M. T.; Graham, R. M. *Mol. Pharmacol.* **1991**, *40*, 876.
10. Schwinn, D. A.; Lomasney, J. M. *Eur. J. Pharmacol.* **1992**, *227*, 433.
11. Hieble, J. P.; Bylund, D. B.; Clarke, A. E.; Eikenberg, D. C.; Langer, S. Z.; Lefkowitz, R. J.; Minneman, K. P.; Ruffolo, R. R. *Pharmacol. Rev.* **1995**, *47*, 267.
12. Flavahan, N. A.; Vanhoutte, P. M. *Trends Pharmacol. Sci.* **1986**, *7*, 347.
13. Muramatsu, I.; Ohmura, T.; Kigoshi, S.; Hashimoto, S.; Oshita M. *Brit. J. Pharmacol.* **1990**, *99*, 197.
14. Muramatsu, I.; Ohmura, T.; Hashimoto, S.; Oshita M. *Mol. Pharmacol. Comm.* **1995**, *6*, 23.
15. De Benedetti, P. G.; Menziani, M. C.; Fanelli, F.; Cocchi, M. *J. Mol. Struct. (Theochem)* **1993**, *285*, 147.
16. Fanelli, F.; Menziani, M. C.; Cocchi, M.; Leonardi, A.; De Benedetti, P. G. *J. Mol. Struct. (Theochem)* **1994**, *314*, 265.
17. Fanelli, F.; Menziani, M. C.; Carotti, A.; De Benedetti, P. G. *Bioorg. Med. Chem.* **1994**, *2*, 195.
18. Menziani, M. C.; Cocchi, M.; Fanelli, F.; De Benedetti, P. G. *J. Mol. Struct. (Theochem)* **1995**, *333*, 243.
19. Menziani, M. C.; Fanelli, F.; Cocchi, M.; De Benedetti, P. G. In *Membrane Protein Models*; Findley, J. B. C., Ed.; BIOS: 1996; p 113.
20. Fanelli, F.; Menziani, M. C.; De Benedetti, P. G. *Bioorg. Med. Chem.* **1995**, *3*, 1465.

21. Savarrese, T. M.; Fraser, C. M. *Biochem. J.* **1992**, 283, 1.
22. Fanelli, F.; Menziani, M. C.; M. Cocchi; De Benedetti, P. G. *J. Mol. Struct. (Theochem)* **1995**, 333, 49.
23. Baldwin, J. M. *EMBO J.* **1993**, 12, 1693.
24. Schertler, G. F. X.; Villa, C.; Henderson, R. *Nature (London)* **1993**, 362, 770.
25. Henderson, R.; Baldwin, J. M.; Ceska, T. A.; Zemlin, F.; Beckmann, E.; Downing, K. H. *J. Mol. Biol.*, **1990**, 213, 899.
26. QUANTA/CHARMm, **1990**, Molecular Simulations, 200 Fifth Avenue, Waltham, MA 02254.
27. Brooks, B. R.; Bruccoleri, R. E.; Olafson, B. D.; States, D. J.; Swaminathan, S.; Karplus, M. *J. Comput. Chem.* **1983**, 4, 187.
28. van Gunsteren, W. F.; Berendsen, J. C. *Mol. Phys.* **1987**, 34, 1311.
29. Dewar, M. J. S.; Zoebisch, E. G.; Healey, E. F.; Stewart, J. J. P. *J. Am. Chem. Soc.* **1985**, 107, 3902.

(Received in U.S.A. 15 August 1996; accepted 5 December 1996)